WILEY-VCH

Extracellular Matrix in Synthetic Hydrogel-based Prostate Cancer Organoids Regulate Therapeutic Response to EZH2 and DRD2 inhibitors

Matthew J Mosquera[1], Sungwoong Kim[2,3], Rohan Bareja[4,5], Zhou Fang[3], Shuangyi Cai[3], Heng Pan[4,5], Muhammad Asad[6], M. Laura Martin[4], Michael Sigouros[4], Florencia M Rowdo[4], Sarah Ackermann[4], Jared Capuano[4], Jacob Bernheim[4], Cynthia Cheung[4], Ashley Doane[4], Nicholas Brady[6], Richa Singh[6], David S. Rickman[6], Varun Prabhu[7], Joshua E Allen[7], Loredana Puca[4], Ahmet Coskun[3], Mark Rubin[8], Himisha Beltran[9], Juan Miguel Mosquera[4,6], Olivier Elemento[4,5], Ankur Singh[1,2,3]**

[1]Sibley School of Mechanical Engineering, Cornell University, Ithaca, NY, USA

[2]Woodruff School of Mechanical Engineering, Georgia Institute of Technology, Atlanta, GA, USA

[3]Coulter Department of Biomedical Engineering, Georgia Institute of Technology and Emory University School of Medicine, Atlanta, GA, USA

[4]Englander Institute for Precision Medicine, Weill Cornell Medicine-New York-Presbyterian Hospital, New York, NY, USA

[5]Institute for Computational Biomedicine, Weill Cornell Medicine, New York, NY, USA

[6]Department of Pathology and Laboratory Medicine, Weill Cornell Medicine, New York, NY, USA

[7]Chimerix, Inc., Durham, NC, USA

[8]Department for BioMedical Research, University of Bern, Bern, Switzerland

[9]Department of Medical Oncology, Dana Farber Cancer Institute, Harvard Medical School, Boston, MA, USA

*Corresponding author: ankur.singh@gatech.edu

*Corresponding author: ole2001@med.cornell.edu

Keywords: epigenetic, dopamine receptor, chemoresistance, neuroendocrine, tumor microenvironment

Supplementary Figure 1
Related to Fig. 1

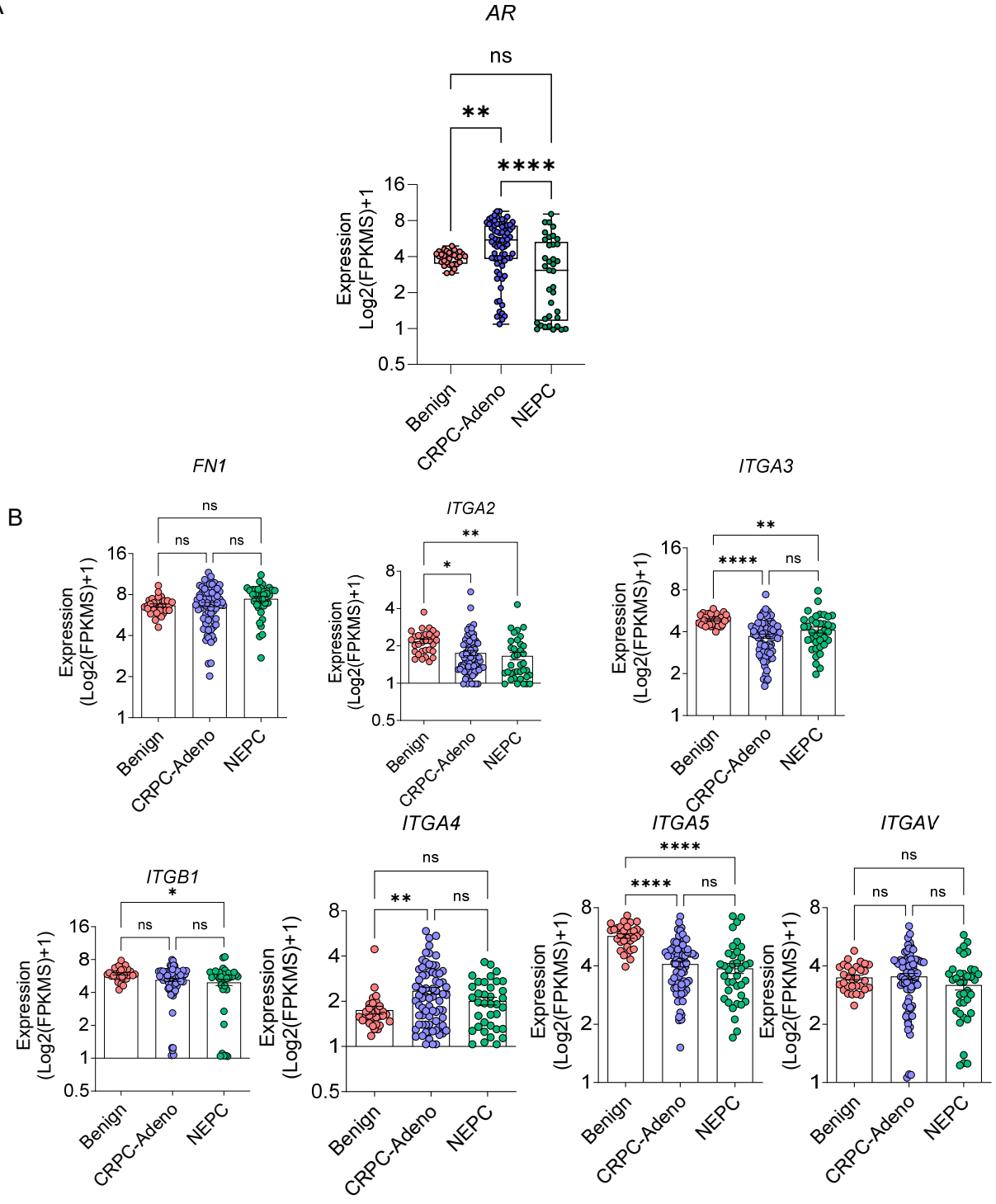

Supplement Figure 1. Patient sample characterization. A) Androgen receptor expression level in CRPC-NEPC patients. **B)** Transcriptomic expression of ECM and integrins across disease state

in the patient cohort. n =31 benign prostate, n =74 CRPC-Adeno, and n =37 CRPC-NEPC. All groups were compared by a one-way ANOVA, with posthoc Tukey's test with *$p<0.05$, ** $p<0.01$, ***$p<0.001$, and ****$p<0.0001$.

Supplementary Figure 2
Related to Fig. 1

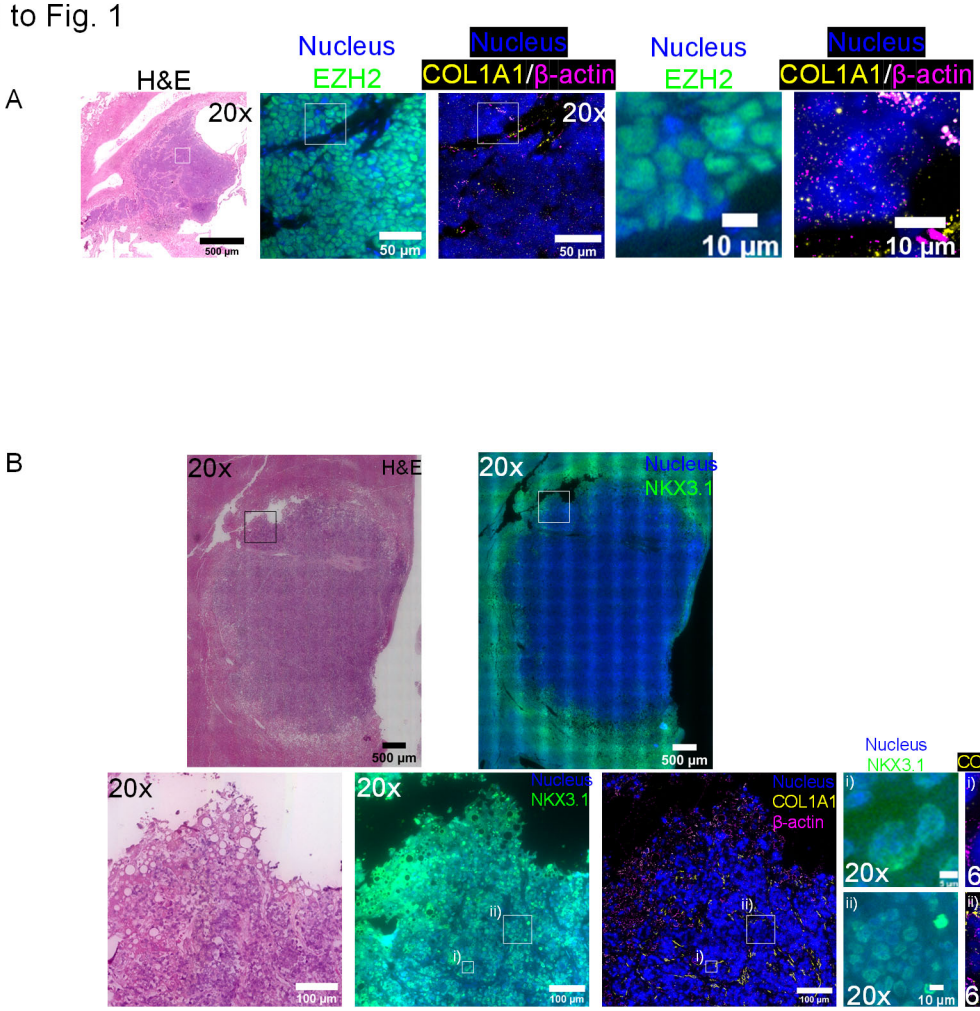

Supplement Figure 2. Multiplexed single-cell analysis and SHG of prostate tumors. A) H&E staining of CRPC-NEPC prostate tumors and immunostaining of EZH2 on CRPC-NEPC prostate tumors. Zoomed in images of single-cell EZH2 distributions (Green) in the second and third rows. Fluorescence in-situ hybridization (FISH) based detection of single COL1A1 AND B-actin RNA molecules in the same area of the CRPC-NEPC prostate tumors using a FISH signal amplification assay, Hybridization Chain Reaction (HCR). Zoomed in images of single-cell RNA distributions of COL1A1 (Yellow) and B-Actin (Magenta) in the second and third rows. Data representative of two patient biopsies. B) H&E staining of CRPC-Adeno prostate tumors and immunostaining of NKX3.1 on CRPC-Adeno prostate tumors. Zoomed in images of single-cell NKX3.1 distributions (Green) in the second and third rows. Fluorescence in-situ hybridization (FISH) based detection of single COL1A1 AND B-actin RNA molecules in the same area of the CRPC-Adeno prostate tumors using a FISH signal amplification assay, Hybridization Chain Reaction (HCR). Zoomed in images of single-cell RNA distributions of COL1A1 (Yellow) and B-Actin (Magenta) in the second and third rows. Data representative of two patient biopsies. C) Second harmonic generation microscopy images of collagen fibers in CRPC-NEPC tissues. The tissue samples were embedded in paraffin and stained with Synaptophysin (SYP). The SHG of tissue samples were imaged on a deparaffinized unstained slide using a two-photon microscope. Data representative of two patient biopsies.

Supplementary Figure 3
Related to Fig. 1

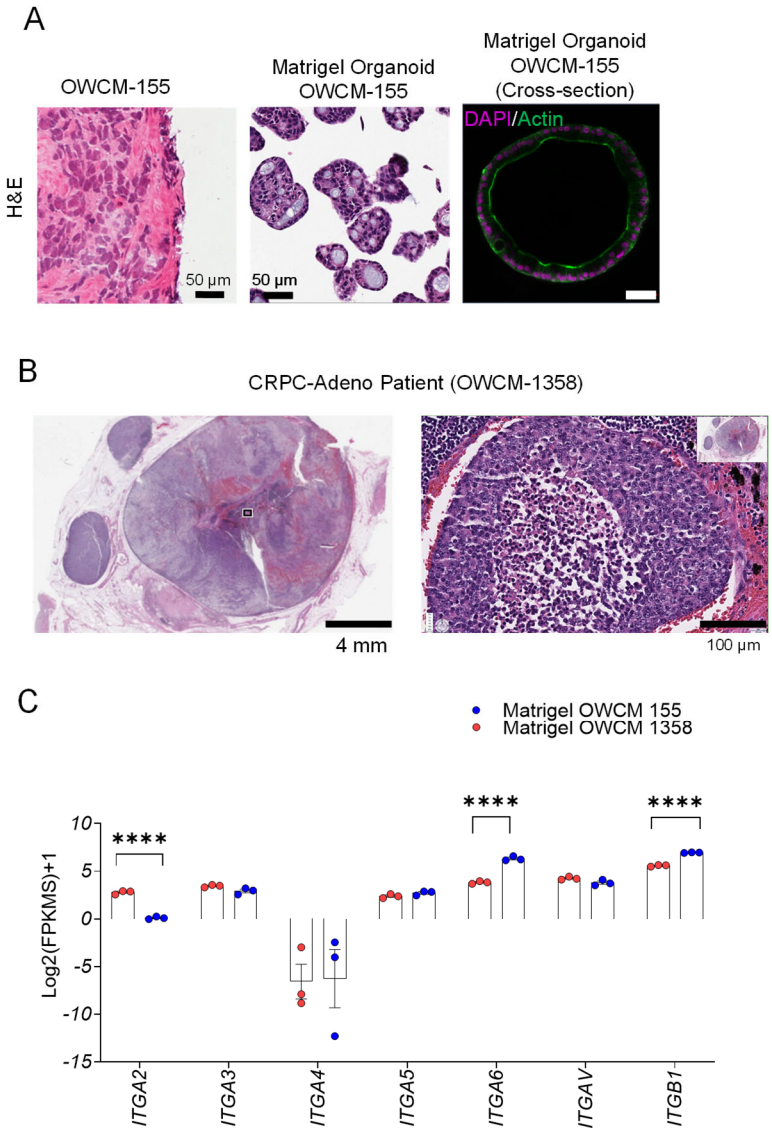

Supplement Figure 2. Characterization of patient tumors and matrigel organoids. A) H&E images of CRPC-NEPC patient OWCM-155, Matrigel organoids of the same patient tumor, and confocal image of OWCM-155 Matrigel organoids.) H&E staining of a rapid autopsy specimen from a single CRPC-Adeno patient. C) Transcriptomic expression of integrins in CRPC-Adeno and CRPC-NEPC matrigel organoids (n =3 each). All groups were compared by a one-way ANOVA, with posthoc Tukey's test (*p<0.05, **p<0.01, ***p<0.001, and ****p<0.0001).

Supplementary Figure 4
Related to Fig. 2

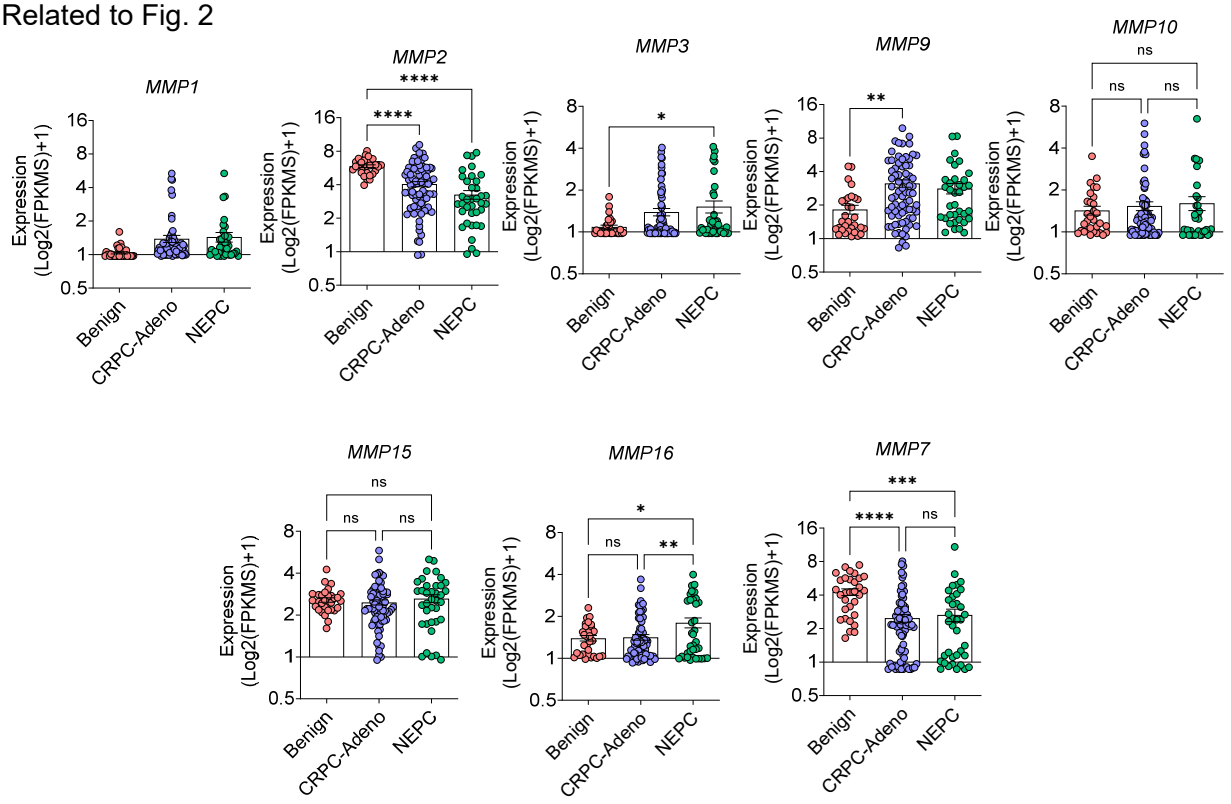

Supplement Figure 4. MMP characterization. Transcriptomic expression of MMPs across disease development in the WCMC patient cohort (n=31 Benign, n=74 CRPC-Adeno, n=37 CRPC-NEPC).

Supplementary Figure 5; Related to Fig. 2

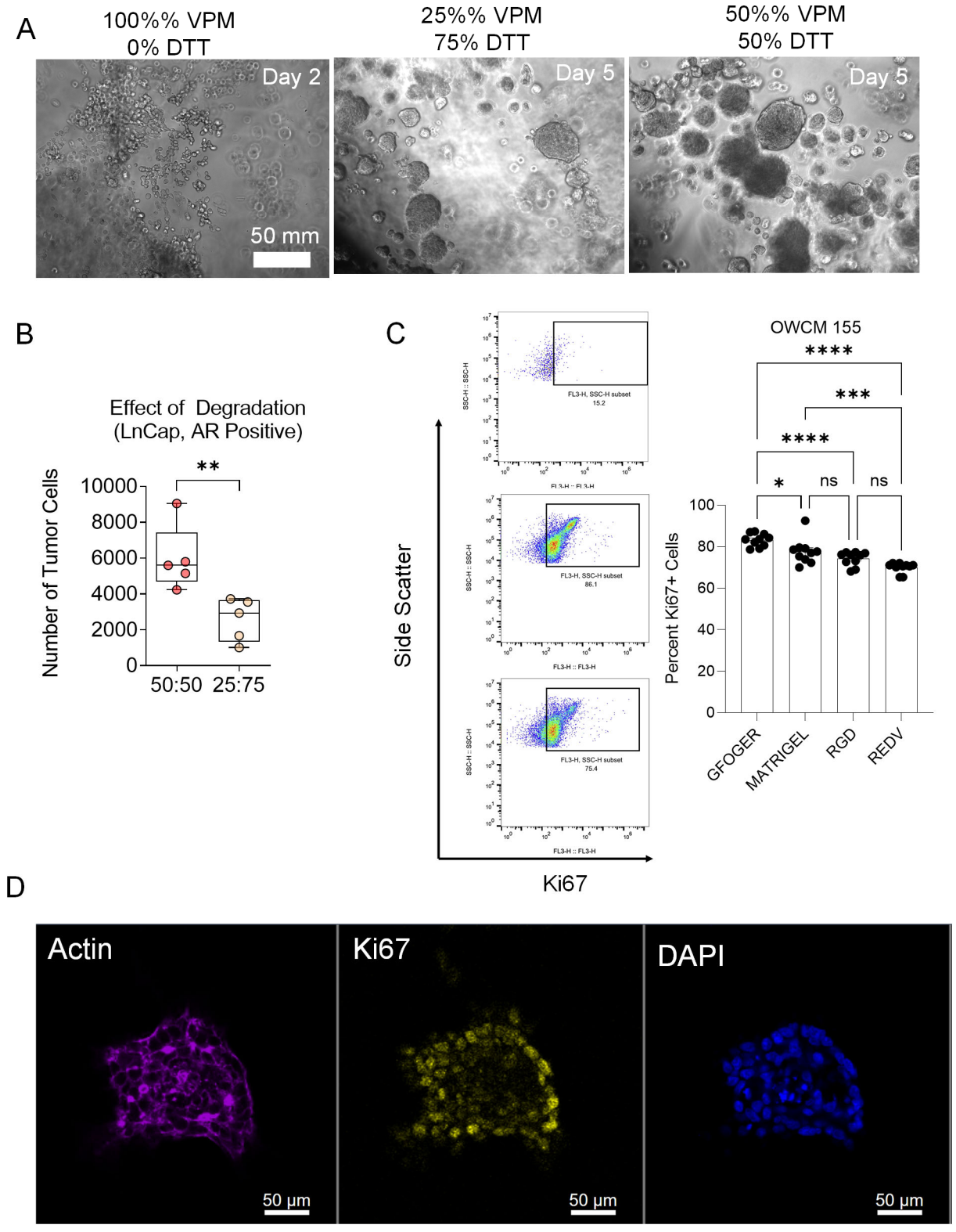

Supplement Figure 5. Organoid characterization. A) Phase-contrast images of PEG-4MAL

hydrogel-based organoids containing LnCap cells. Hydrogel were crosslinked with varying ratio of VPM and DTT to modulate degradation. **B**) Effect of degradation rate on growth of synthetic organoids containing LnCap cells (n=5). All groups were compared by an unpaired, two-tailed, t-test with *p<0.05, ** p<0.01, ***p<0.001, and ****p<0.0001. **C**) Effect of ECM type on Ki67 expression in OWCM-155 tumors grown in synthetic hydrogel-based or Matrigel organoids (n=10).). All groups were compared by a one-way ANOVA, with posthoc Tukey's test (*p<0.05, **p<0.01, ***p<0.001, and ****p<0.0001). **D**) Confocal image of Ki67 expression in REDV-functionalized PEG-4MAL hydrogel organoid.

Supplementary Figure 6
Related to Fig. 2

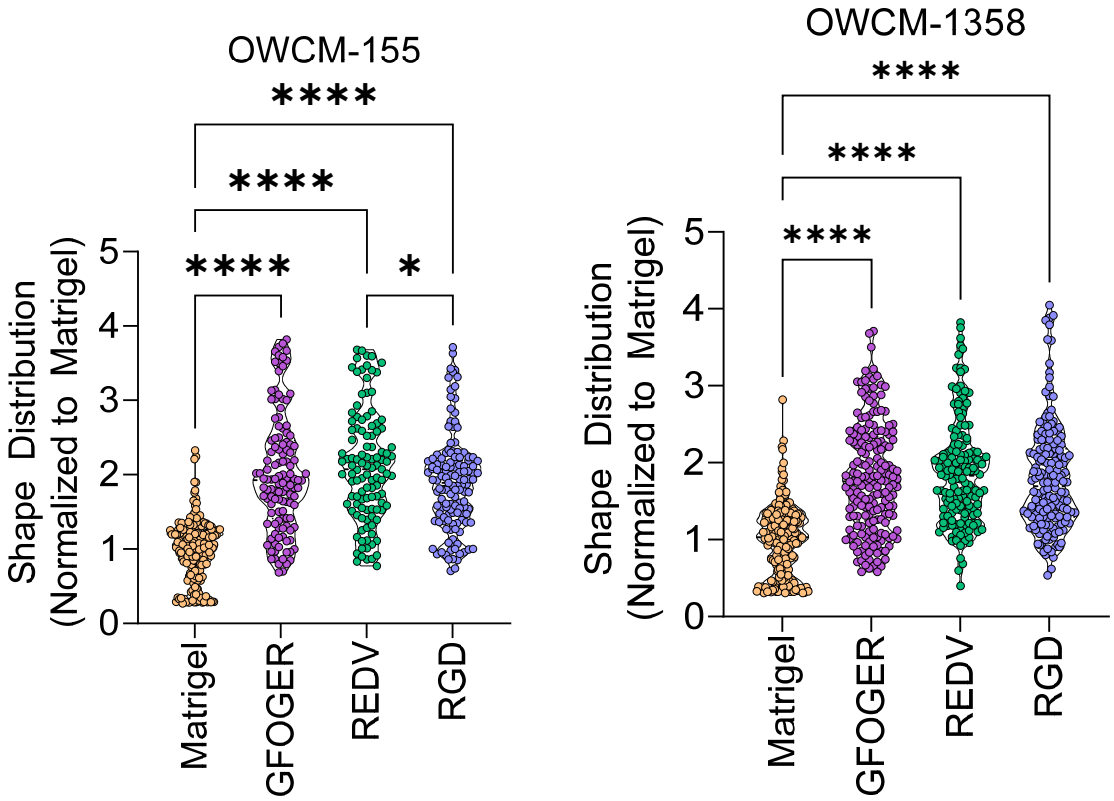

Supplement Figure 6. **Organoid characterization.** High content image analysis of prostate organoid shape distribution across ECM conditions in OWCM-155 (Matrigel n=204, RGD n=135, REDV n=113, GFOGER n=123 cell clusters, N =5 organoids each) and OWCM-1258 organoids (n=206 Matrigel, n=167 RGD, n=158 REDV, n=187 GFOGER). Groups were compared by a one-

way ANOVA, with posthoc Tukey's test with ****p<0.0001.

Supplementary Figure 7
Related to Fig. 2

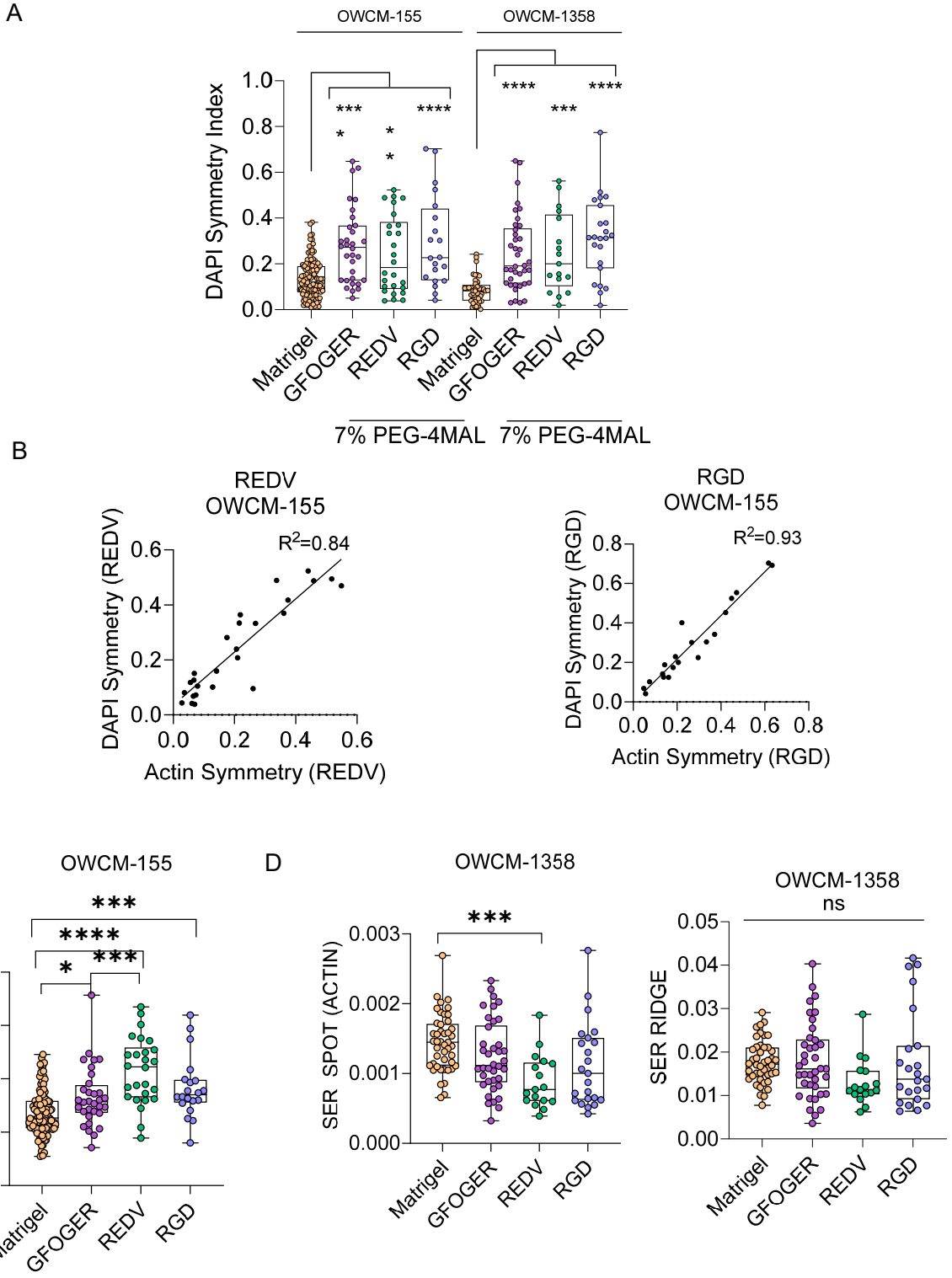

Supplement Figure 7. Organoid characterization. A) High content imaging characterizes nuclear morphology. (CRPC-NEPC: Matrigel n=128, GFOGER n=32, REDV n=26, RGD n=20. CRPC-Adeno: Matrigel n=45, GFOGER n=38, REDV n=17, RGD n=23). CRPC-NEPC and CRPC-Adeno organoids were compared by a one-way ANOVA, with post-hoc Tukey's test with **p<0.01, ***p<0.001, and ****p<0.0001. **B)** Correlation analysis between Actin and DAPI symmetry among REDV (left) and RGD (right) organoids (n=26 REDV, n= 20 RGD). **C)** High content imaging for texture analysis of actin SPOT values among CRPC-Adeno organoids (Matrigel n=45, GFOGER n=38, REDV n=17, RGD n=23). **D)** High content imaging analysis of actin RIDGE values among CRPC-NEPC (left) and CRPC-Adeno (right) organoids. For all groups, comparisons were made with a one-way ANOVA with posthoc Tukey's test with *p<0.05, **p<0.01, ***p<0.001, and ****p<0.0001.

Supplementary Figure 8
Related to Fig. 3

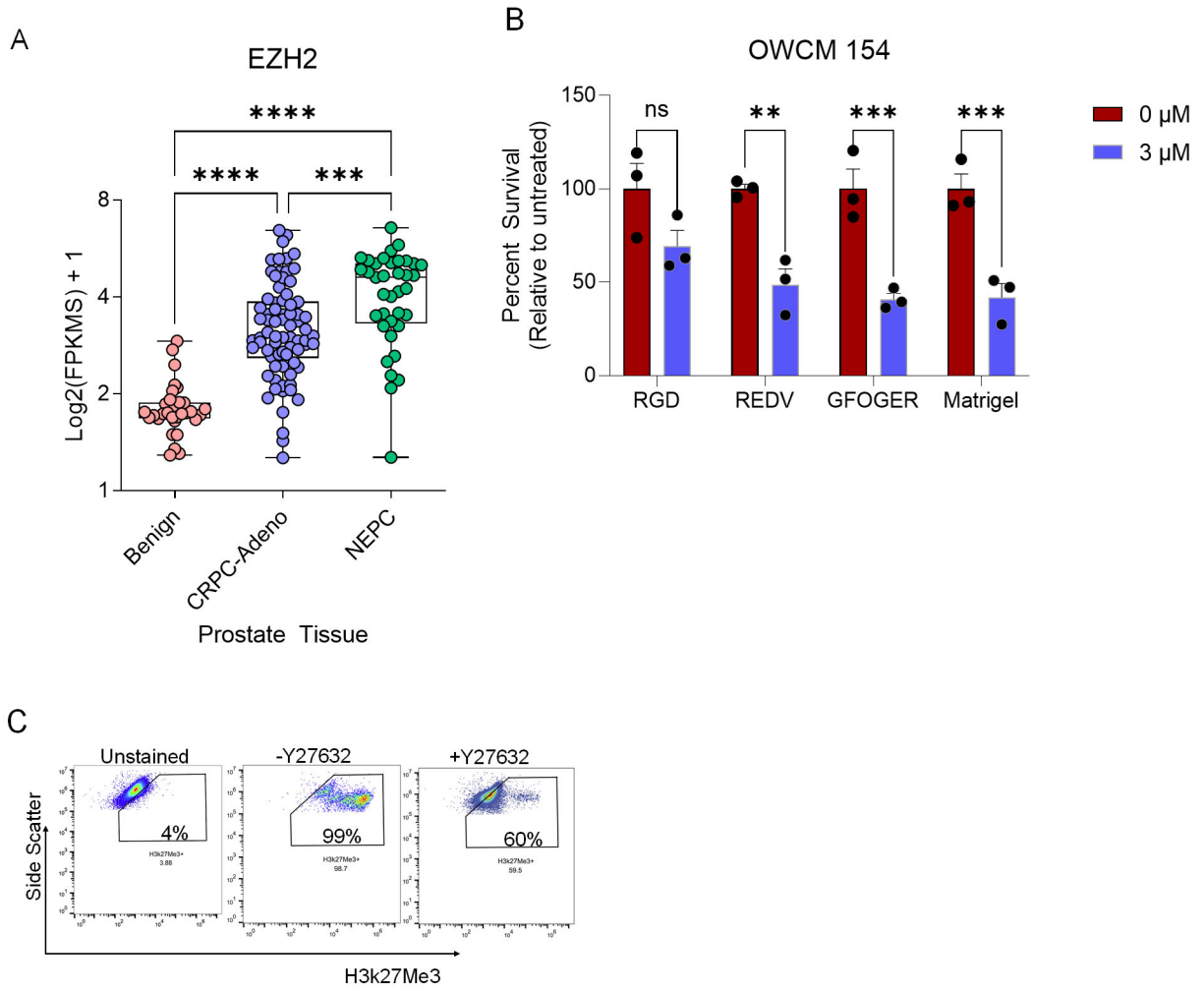

Supplement Figure 8. Patient tumors and Organoid Characterization. A) Transcriptomic analysis of EZH2 across patient subtypes during disease progression (Benign Prostate n=29, CRPC-Adeno n=66, CRPC-NEPC n=36, Matrigel n=10). **B)** Fold change in OWCM-154 organoid growth area under treatment with an EZH2i GSK343. N =3; a two-tailed t-test evaluated each treated and untreated comparisons with *p<0.05 and ****p<0.0001. **C**) Gating schematic for Y27632 analysis of H3k27Me3.

Supplementary Figure 9
Related to Fig. 4

A

ENTREZID	SD	SYMBOL
338657	0.459148885	CCDC84
8358	0.378880615	HIST1H3B
8335	0.368405853	HIST1H2AI
8031	0.355716429	NCOA4
2842	0.339538849	GPR19
1E+08	0.337762951	LOC10024
129049	0.337385822	SGSM1
3481	0.335933368	IGF2
4504	0.319926559	MT3
644961	0.319653917	ACTG1P20
23081	0.319157434	KDM4C
9326	0.316186512	ZNHIT3
147872	0.312234148	CCDC155
5608	0.308469241	MAP2K6
1E+08	0.304830714	ZNF37BP
27289	0.304635795	RND1
170393	0.302342343	C10orf91
151507	0.300088151	MSL3P1
1.01E+08	0.296549863	MIR3908
10188	0.290460929	TNK2
440823	0.289665252	MIAT
4893	0.288408823	NRAS
727936	0.288240182	GXYLT2
79608	0.285273261	RIC3
8631	0.281817823	SKAP1
79736	0.280246082	TEFM
11144	0.278859991	DMC1
8929	0.276651475	PHOX2B
9564	0.273153903	BCAR1
116115	0.26926722	ZNF526
162989	0.26425354	DEDD2
221409	0.263377105	SPATS1
255349	0.263000849	TMEM211
125476	0.261052206	INO80C
113878	0.259273122	DTX2
650669	0.259151597	GAS6-AS1
64897	0.258391918	C12orf43
326625	0.257876439	MMAB
51433	0.248550568	ANAPC5
3694	0.248003732	ITGB6
126003	0.246982564	TRAPPC5
23229	0.246903853	ARHGEF9
4598	0.245726746	MVK
344657	0.245569091	LRRIQ4
119395	0.244392959	CALHM3
91351	0.244182703	DDX60L
64114	0.243558294	TMBIM1
399947	0.241382319	C11orf87
5201	0.240755175	PFDN1
2876	0.239914196	GPX1
84771	0.239149222	DDX11L2
1E+08	0.237129329	MIR1468
58509	0.237085256	CACTIN
338699	0.23522083	ANKRD42
83550	0.234131484	GPR101
203238	0.233398211	CCDC171
4637	0.231591231	MYL6
23636	0.231470456	NUP62
259307	0.231470456	IL4I1
121456	0.231033149	SLC9A7P1
7177	0.229000131	TPSAB1
54929	0.228645311	TMEM161
3615	0.228243893	IMPDH2
158724	0.227144027	FAM47A
112724	0.226910469	RDH13
11082	0.226821756	ESM1
137872	0.22651544	ADHFE1
5985	0.225373614	RFC5
9488	0.225151594	PIGB
128822	0.224742173	CST9
2001	0.224699443	ELF5
84519	0.223482579	ACRBP
151903	0.223364219	CCDC12
150291	0.220533734	MORC2-AS
7368	0.22053352	UGT8
55230	0.220435785	USP40
2743	0.220315371	GLRB
55286	0.219787489	C4orf19
84282	0.219455037	RNF135
9349	0.219266082	RPL23
345930	0.217050099	ECT2L
55101	0.216853223	ATP5SL
286207	0.216825265	CFAP157
54980	0.216644242	C2orf42
10411	0.215165802	RAPGEF3
57521	0.215154596	RPTOR
9175	0.214922083	MAP3K13
56104	0.213855468	PCDHGB1
8563	0.213747655	THOC5
6120	0.213243948	RPE
134111	0.213194015	UBE2QL1
252948	0.212816527	TTTY16
256435	0.212716203	ST6GALNA
246213	0.211530033	SLC17A8
54857	0.210683734	GDPD2
2645	0.210593731	GCK
8755	0.210409479	ADAM6
51128	0.210366969	SAR1B
221806	0.209606094	VWDE
339456	0.209512194	TMEM52

B

	AR		KLK3		ENO2		NKX3-1		ARV7		CHGA		SYP		FOLH1 (PSM)	
	CRPC NEPC		CRPC NEPC		CRPC NEPC		CRPC NEPC		CRPC NEPC		CRPC NEPC		CRPC NEPC		CRPC NEPC	
	log2FoldChange	pvalue	log2FoldChange	pvalue	log2FoldChange	pvalue	log2FoldChange	pvalue	log2FoldChange	pvalue	log2FoldChange	pvalue	log2FoldChange	pvalue	log2FoldChange	pvalue
RGD	#N/A	#N/A	#N/A	#N/A	0.104994	0.532742	-0.16896	0.446354	#N/A	#N/A	0.601702	0.431524	0.03287	0.922316	0.286756	0.279733
REDV	#N/A	#N/A	#N/A	#N/A	-0.08159	0.533777	-0.1519	0.388967	#N/A	#N/A	-0.02633	0.869442	-0.33927	0.037969	0.372935	0.038219
GFOGER	#N/A	#N/A	#N/A	#N/A	-0.11749	0.323558	-0.09705	0.574255	#N/A	#N/A	-0.03255	0.81953	-0.28632	0.058582	0.219247	0.219479

C

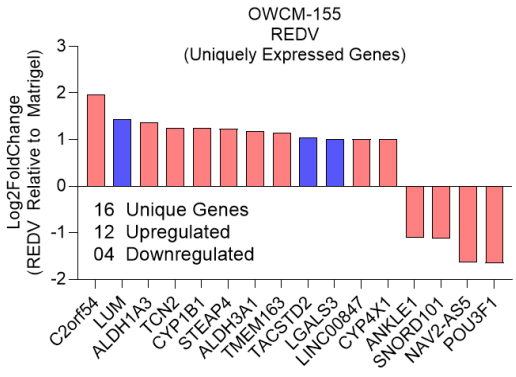

Supplementary Figure 9. DNA Methylation and RNA-seq analysis. A) List of the top 100 most variable promoters of methylation. This analysis is based on the standard deviation of promoter

methylation across all the samples. **B)** Relative change in hallmark prostate cancer genes in various ECM conditions relative to Matrigel. **C)** Unique genes expressed by OWCM-155 tumors grown in REDV hydrogels. Blue indicated genes that are related to cell adhesion or cytoskeletal pathways.

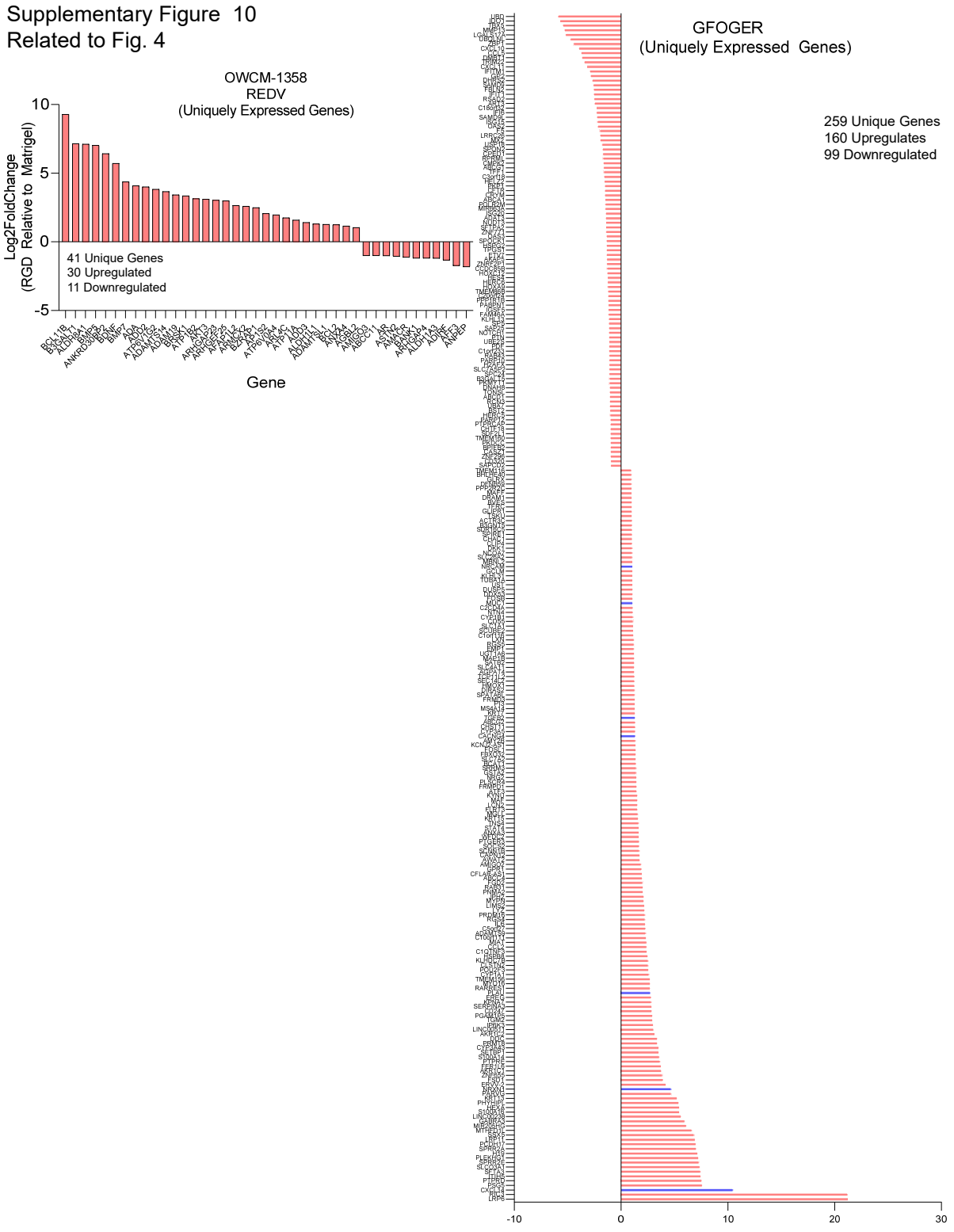

Supplementary Figure 10. Uniquely expressed genes in REDV and GFOGER-functionalized PEG-4MAL-based organoids in CRPC-Adeno. (n=3 per condition). Blue indicates genes that are

related to cell adhesion or cytoskeletal pathways.

Supplementary Figure 11
Related to Fig. 5

OWCM-155
(RGD vs Matrigel)

	GS follow link to MSigDB	GS DETAILS	SIZE	ES	NES	NOM p-val	FDR q-val	FWER p-val	RANK AT MAX	LEADING EDGE
1	GO:0031012	Details ...	192	0.65	1.71	0.000	0.001	0.001	2921	tags=53%, list=19%, signal=65%
2	GO:0007155	Details ...	459	0.53	1.43	0.000	0.040	0.079	2766	tags=34%, list=18%, signal=40%
3	GO:0007389	Details ...	41	0.52	1.27	0.119	0.093	0.254	3726	tags=39%, list=24%, signal=51%
4	GO:0043565	Details ...	364	0.40	1.08	0.220	0.363	0.813	4374	tags=37%, list=29%, signal=51%
5	GO:0048598	Details ...	19	0.48	1.07	0.409	0.301	0.825	3504	tags=32%, list=23%, signal=41%

Upregulated Genesets

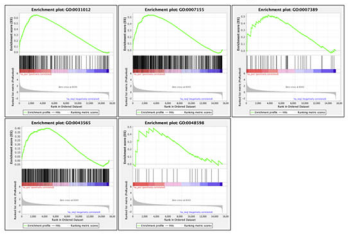

OWCM-155
(REDV vs Matrigel)

	GS follow link to MSigDB	GS DETAILS	SIZE	ES	NES	NOM p-val	FDR q-val	FWER p-val	RANK AT MAX	LEADING EDGE
1	GO:0031012	Details ...	187	0.53	1.76	0.000	0.002	0.002	2742	tags=45%, list=18%, signal=55%
2	GO:0007155	Details ...	453	0.49	1.75	0.000	0.001	0.002	2215	tags=31%, list=14%, signal=35%
3	GO:0007389	Details ...	42	0.48	1.34	0.118	0.071	0.205	1842	tags=33%, list=12%, signal=38%
4	GO:0043565	Details ...	364	0.27	0.94	0.644	0.605	0.966	2525	tags=19%, list=17%, signal=22%

Upregulated Genesets

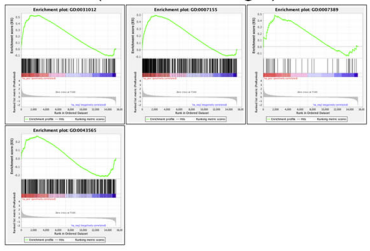

	GS follow link to MSigDB	GS DETAILS	SIZE	ES	NES	NOM p-val	FDR q-val	FWER p-val	RANK AT MAX	LEADING EDGE
1	GO:0048598	Details ...	19	-0.28	-0.73	0.842	0.910	0.667	59	tags=5%, list=0%, signal=5%

Downregulated Genesets

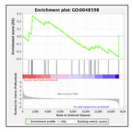

OWCM-155
(GFOGER vs Matrigel)

	GS follow link to MSigDB	GS DETAILS	SIZE	ES	NES	NOM p-val	FDR q-val	FWER p-val	RANK AT MAX	LEADING EDGE
1	GO:0031012	Details ...	180	0.51	1.80	0.000	0.000	0.000	1467	tags=34%, list=10%, signal=37%
2	GO:0007155	Details ...	443	0.46	1.75	0.000	0.001	0.001	2138	tags=30%, list=14%, signal=35%
3	GO:0007389	Details ...	40	0.36	1.00	0.451	0.616	0.854	2198	tags=33%, list=15%, signal=38%
4	GO:0048598	Details ...	19	0.30	0.71	0.855	0.957	0.996	2019	tags=21%, list=14%, signal=24%

Upregulated Genesets

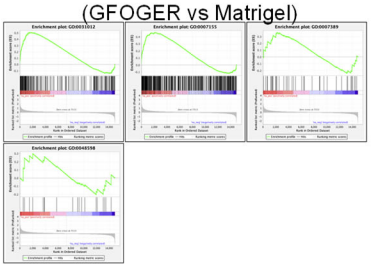

	GS follow link to MSigDB	GS DETAILS	SIZE	ES	NES	NOM p-val	FDR q-val	FWER p-val	RANK AT MAX	LEADING EDGE
1	GO:0043565	Details ...	353	-0.31	-1.30	0.004	0.082	0.124	2174	tags=20%, list=15%, signal=23%

Downregulated Genesets

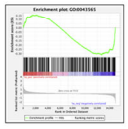

Continued Supplementary Figure 11
Related to Fig. 5

OWCM-155
(RGD vs Matrigel)

	GS follow link to MSigDB	GS DETAILS	SIZE	ES	NES	NOM p-val	FDR q-val	FWER p-val	RANK AT MAX	LEADING EDGE
1	LI_PROSTATE_CANCER_EPIGENETIC	Details ...	25	0.73	1.67	0.000	0.001	0.001	2491	tags=56%, list=16%, signal=67%
2	EXTRACELLULAR_MATRIX	Details ...	72	0.63	1.62	0.000	0.004	0.007	2939	tags=53%, list=19%, signal=65%
3	HALLMARK_EPITHELIAL_MESENCHYMAL_TRANSITION	Details ...	169	0.59	1.55	0.000	0.006	0.017	2921	tags=44%, list=19%, signal=54%
4	KEGG_ECM_RECEPTOR_INTERACTION	Details ...	71	0.59	1.49	0.003	0.018	0.068	2546	tags=44%, list=17%, signal=52%
5	GO_NEUROENDOCRINE_CELL_DIFFERENTIATION	Details ...	8	0.68	1.27	0.180	0.139	0.490	233	tags=25%, list=2%, signal=25%
6	REACTOME_INTEGRIN_SIGNALING	Details ...	24	0.54	1.23	0.189	0.167	0.632	1544	tags=21%, list=10%, signal=23%
7	KONDO_EZH2_TARGETS	Details ...	171	0.46	1.20	0.074	0.182	0.722	2955	tags=28%, list=19%, signal=34%
8	KEGG_PROSTATE_CANCER	Details ...	79	0.29	0.74	0.898	0.886	1.000	4681	tags=28%, list=31%, signal=40%

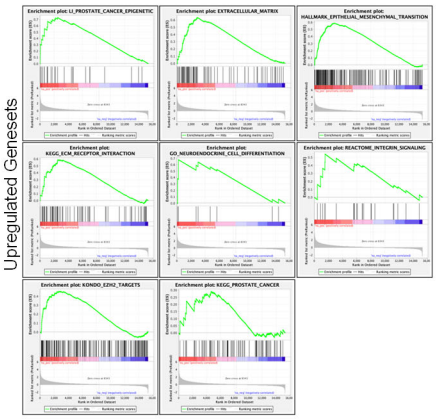

OWCM-155
(REDV vs Matrigel)

	GS follow link to MSigDB	GS DETAILS	SIZE	ES	NES	NOM p-val	FDR q-val	FWER p-val	RANK AT MAX	LEADING EDGE
1	HALLMARK_EPITHELIAL_MESENCHYMAL_TRANSITION	Details ...	169	0.56	1.83	0.000	0.001	0.001	2476	tags=37%, list=16%, signal=44%
2	LI_PROSTATE_CANCER_EPIGENETIC	Details ...	24	0.69	1.69	0.011	0.009	0.012	1796	tags=46%, list=12%, signal=52%
3	KEGG_ECM_RECEPTOR_INTERACTION	Details ...	70	0.56	1.66	0.001	0.009	0.020	2174	tags=37%, list=14%, signal=43%
4	KONDO_EZH2_TARGETS	Details ...	177	0.48	1.59	0.000	0.019	0.058	1865	tags=25%, list=12%, signal=29%
5	EXTRACELLULAR_MATRIX	Details ...	69	0.50	1.49	0.034	0.043	0.151	2831	tags=45%, list=19%, signal=55%
6	GO_NEUROENDOCRINE_CELL_DIFFERENTIATION	Details ...	8	0.70	1.36	0.120	0.094	0.345	1850	tags=50%, list=12%, signal=57%
7	REACTOME_INTEGRIN_SIGNALING	Details ...	24	0.47	1.16	0.290	0.277	0.788	3670	tags=33%, list=24%, signal=44%
8	KEGG_PROSTATE_CANCER	Details ...	80	0.22	0.68	0.973	0.941	1.000	3583	tags=20%, list=23%, signal=26%

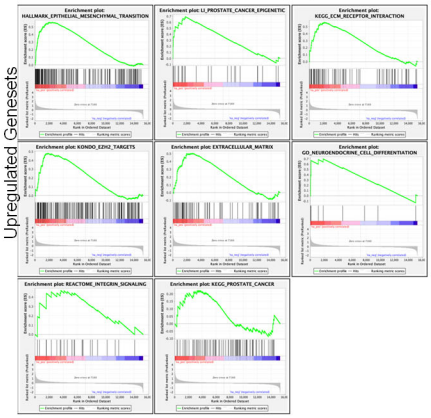

OWCM-155
(GFOGER vs Matrigel)

	GS follow link to MSigDB	GS DETAILS	SIZE	ES	NES	NOM p-val	FDR q-val	FWER p-val	RANK AT MAX	LEADING EDGE
1	HALLMARK_EPITHELIAL_MESENCHYMAL_TRANSITION	Details ...	167	0.53	1.84	0.000	0.006	0.005	2068	tags=36%, list=14%, signal=41%
2	KEGG_ECM_RECEPTOR_INTERACTION	Details ...	69	0.55	1.73	0.002	0.007	0.010	2040	tags=39%, list=14%, signal=45%
3	LI_PROSTATE_CANCER_EPIGENETIC	Details ...	24	0.64	1.63	0.012	0.017	0.031	1726	tags=46%, list=12%, signal=52%
4	EXTRACELLULAR_MATRIX	Details ...	68	0.48	1.49	0.021	0.046	0.108	2720	tags=44%, list=18%, signal=54%
5	GO_NEUROENDOCRINE_CELL_DIFFERENTIATION	Details ...	7	0.75	1.44	0.083	0.053	0.156	120	tags=29%, list=1%, signal=29%
6	KONDO_EZH2_TARGETS	Details ...	176	0.41	1.44	0.004	0.045	0.158	2058	tags=27%, list=14%, signal=31%
7	REACTOME_INTEGRIN_SIGNALING	Details ...	24	0.42	1.09	0.355	0.360	0.810	1451	tags=17%, list=10%, signal=18%
8	KEGG_PROSTATE_CANCER	Details ...	80	0.21	0.68	0.964	0.950	1.000	1939	tags=11%, list=13%, signal=13%

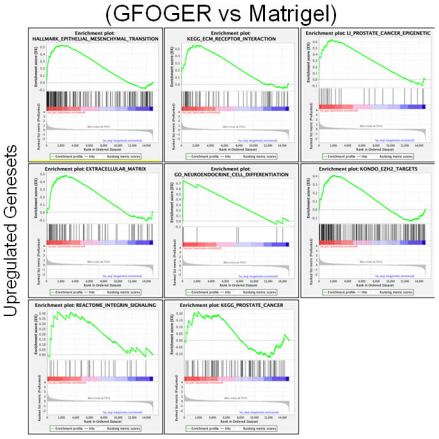

Continued Supplementary Figure 11
Related to Fig. 5

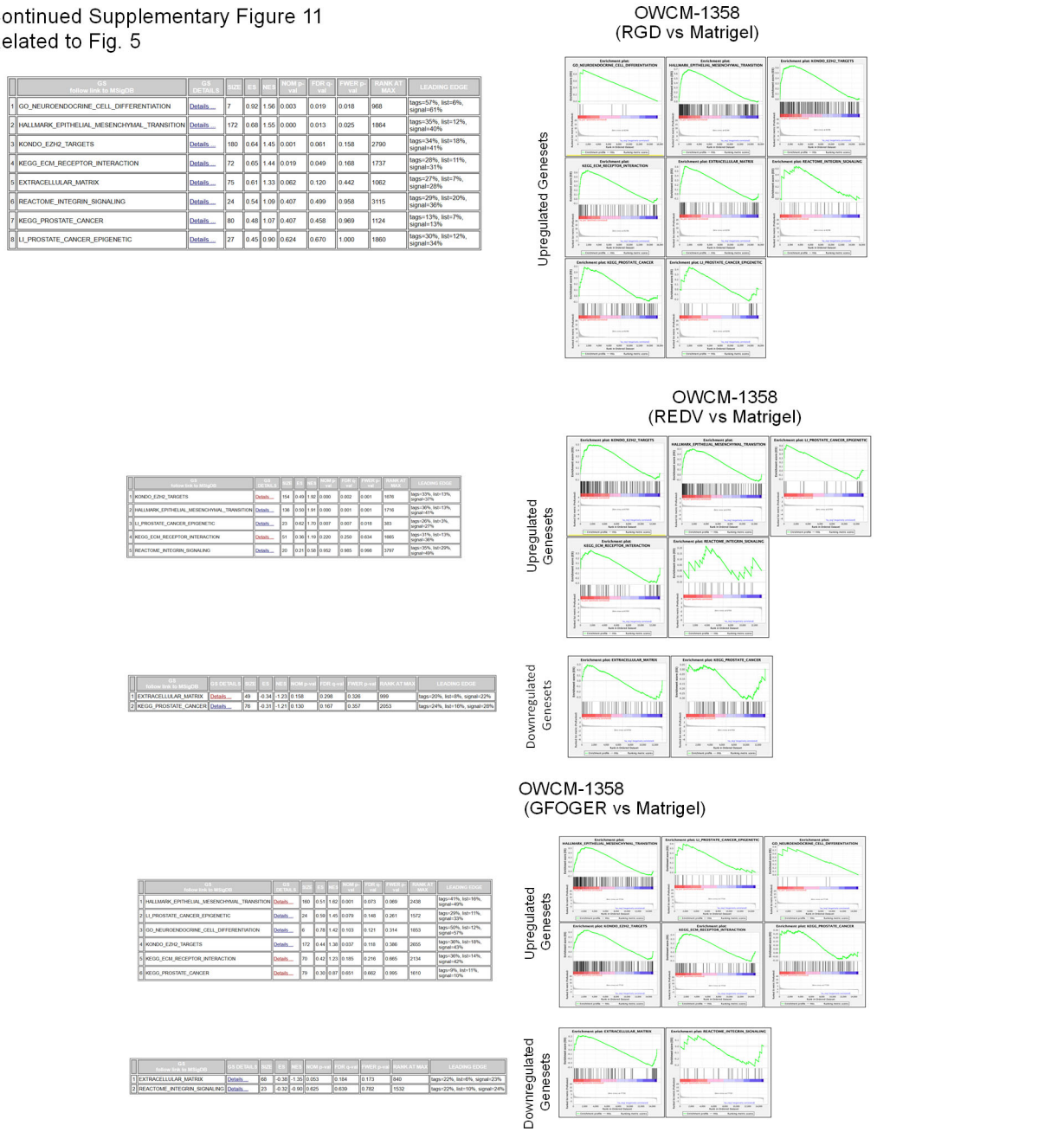

Supplementary Figure 11. GSEA analysis of differential regulation of genesets in CRPC-NEPC and CRPC-Adeno organpoids (n=3 per condition)

Supplementary Figure 12
Related to Fig. 5

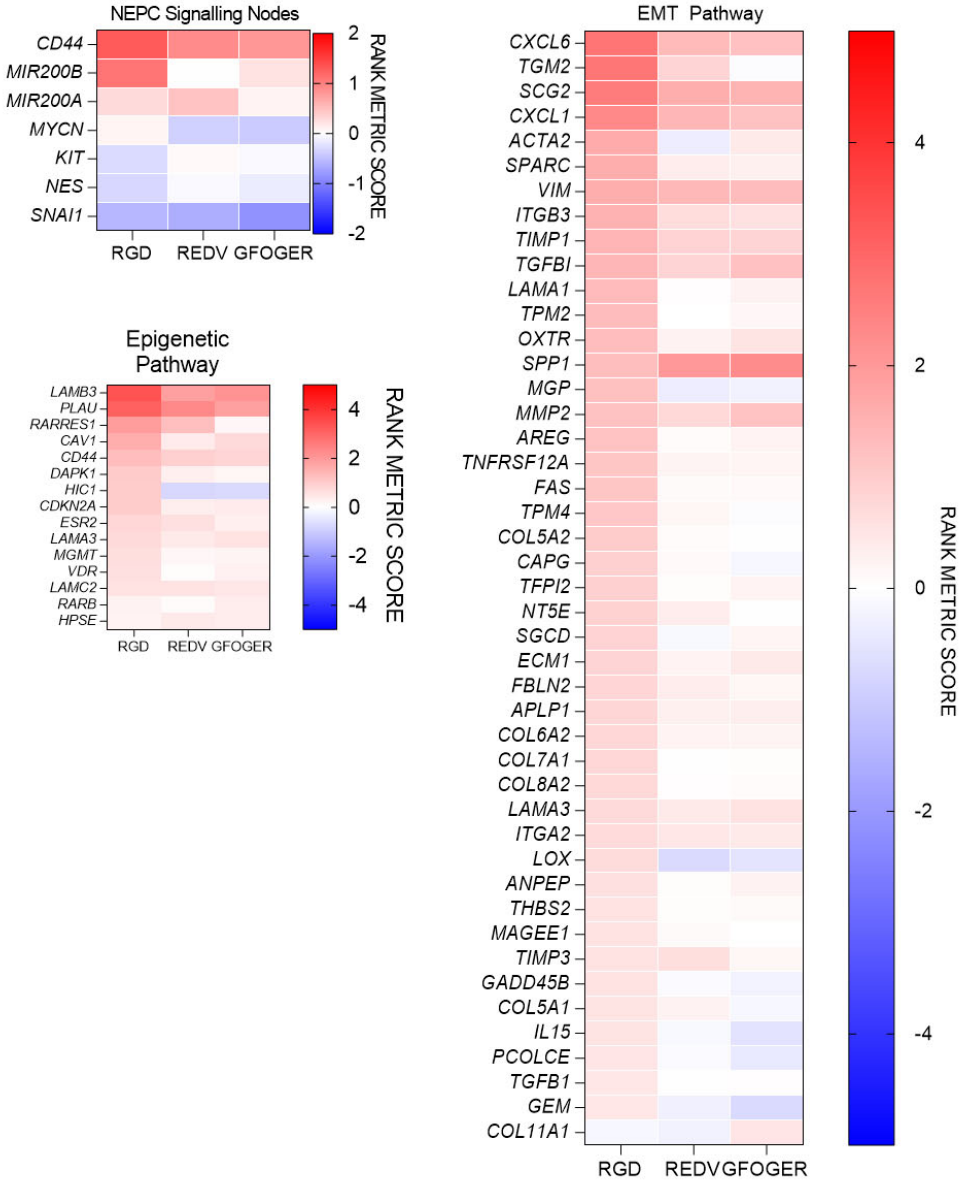

Supplementary Figure 12. GSEA analysis of differential regulation of genesets in CRPC-NEPC OWCM-155 organoids (n=3 per condition)

Supplementary Figure 13
Related to Fig. 5

OWCM-1358

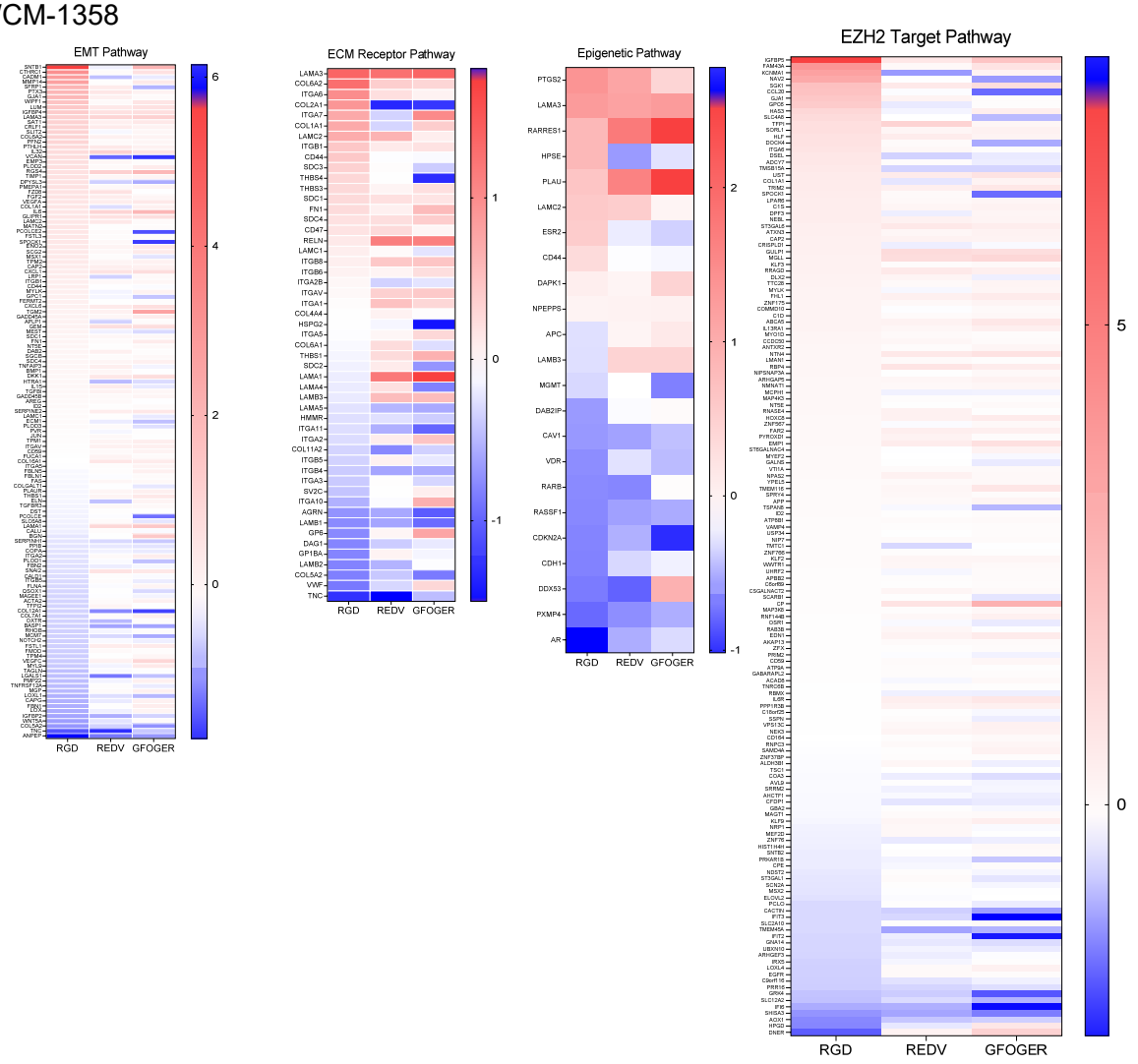

Supplementary Figure 13. GSEA analysis of differential regulation of genesets in CRPC-Adeno OWCM-1358 organoids (n=3 per condition)

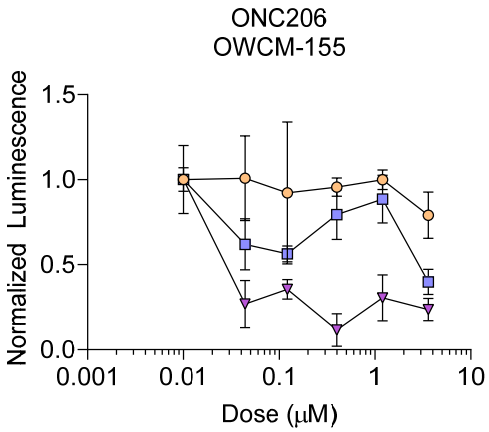

Supplementary Figure 14. Drug response curves in OWCM-155 organoids for ONC206 treatment with and without EZH2 inhibitor, GSK343 (n=5 per condition). Each growth condition was normalized to untreated conditions for that group.

Antibody	Vendor	Catalog	Clone
CD29	Epitomics	1798-1	EP1041Y
EZH2	BD Biosciences	612666	11/EZH2
Goat anti-Rabbit IgG (H+L) Highly Cross-Adsorbed Secondary Antibody, Alexa Fluor 488	Thermo Fisher Scientific	A-11034	N/A
Goat anti-Mouse IgG (H+L) Superclonal™ Secondary Antibody, Alexa Fluor 555	Thermo Fisher Scientific	A-28180	N/A
Integrin alpha-2	Abcam	ab133557	EPR5788
Alexa Fluor 647 anti-mouse/human Ki-67	BioLegend	151206	11F6
NKX3.1	Biocare Medical	CP422A	N/A
Alexa Fluor 488 Phalloidin	Cell Signaling Technology	8878S	N/A
Synaptophysin	Leica	PA0299	27G12
Tri Methyl Histone H3 (Lys27)	Cell Signaling Technology	9733S	C36B11
Vimentin Alexa Fluor 647	Thermo Fisher Scientific	MA5-11883-A647	V9
EZH2	Abcam	ab231165	EPR9307(2)
H3K27me3	Cell signaling Technology	9733BF	C36B11
Anti-rabbit IgG (H+L), F(ab')2 Fragment (Alexa Fluor® 488 Conjugate)	Cell signaling Technology	4412	

Supplementary Figure 14. Antibodies used in studies.